AJNR

Percutaneous Translumbar Spinal Cord Compression Injury in Dogs from an Angioplasty Balloon: MR and Histopathologic Changes with Balloon Sizes and Compression Times

Phillip D. Purdy, Charles L. White III, Donna L. Baer, William H. Frawley, R. Ross Reichard, G. Lee Pride, Jr, Christina Adams, Susan Miller, Christa L. Hladik and Zerrin Yetkin

Percutaneous Translumbar Spinal Cord Compression Injury in Dogs from an Angioplasty Balloon: MR and Histopathologic Changes with Balloon Sizes and Compression Times

Phillip D. Purdy, Charles L. White III, Donna L. Baer, William H. Frawley, R. Ross Reichard, G. Lee Pride, Jr, Christina Adams, Susan Miller, Christa L. Hladik, and Zerrin Yetkin

BACKGROUND AND PURPOSE: Our previous model of spinal cord injury (SCI) included six dogs undergoing 30-minute compression with a balloon in the subarachnoid space. We determined whether various balloon sizes and compression times creates a gradation of injuries.

METHODS: In 17 dogs (including our original six), angioplasty balloons 2, 4, or 7 mm in diameter (2 cm long) were inflated at T6 for 30, 120, or 240 minutes. T1- and T2-weighted, gadolinium-enhanced, and short-tau inversion recovery (STIR) MR images were obtained at 1.5 T. Spinal canal occlusion (SCO) was measured as balloon area–spinal cord area. Hematoxylin-eosin and beta amyloid precursor protein staining were performed to demonstrate hemorrhage and axonal injury, respectively. Injuries were scored as mild, moderate, or severe. Trends were assessed with one-way analysis of variance.

RESULTS: SCO was 12.5–20% for 2-mm balloons, 28–56% for 4 mm, and 62–82% for 7 mm. No abnormalities were seen with SCO <30%. T1- and T2-weighted images had the poorest diagnostic performance; STIR images were best for predicting hemorrhage and axonal injury. Hemorrhage was demonstrated more frequently than was axonal injury. SCO ($P < .0001$) and hemorrhage ($P = .002$) significantly increased with balloon size. Longer inflation times tended to increase injuries for a given size, but differences were not significant.

CONCLUSION: Compression injuries depended on the level of SCO. The compression times tested had less effect than the degree of compression. The value of 1.5-T MR imaging varied with the sequence and improved with contrast enhancement. STIR images showed SCIs not otherwise detected.

The pathophysiology of spinal cord injury (SCI) has been investigated by using various experimental mod-

els such as weight drop (1), pneumatic impaction (2–4), and extradural balloon compression (5). However, the multifactorial nature of human SCI and the multitude investigations and treatments necessitate the development of models that optimize studies of differing aspects of SCI (6). The recent popularity and widespread use of the impact model for SCI, first described by Allen in 1911 (1), has substantially improved our understanding of the neuropathologic processes in subjects with rapid acceleration-deceleration or projectile injury and, by inference, the broader spectrum of SCI. However, inherent to that model is a surgical procedure (laminectomy) and exposure of the spinal column to air, and these are

not characteristic of injuries occurring in natural circumstances.

The current emphasis on rodent models is both economical and less controversial than others, but it has drawbacks in its applicability to commonly used clinical imaging tools (eg, meter-bore 1.5-T MR units). Rodent spinal cords are smaller than human spinal cords, and in humans, the histopathology of injury reflects a wide spectrum of hemorrhagic and axonal findings that are often patchy and that vary from one subject to the next. Also, some have suggested the possibility of anatomically different CSF circulations between rats and humans (7).

The weight-drop model has made important contributions to our understanding of SCI, many of these were referenced in our earlier report (8). Some investigators have shown similarities between the weight-drop model in rodents and human SCI using motor evoked potentials and somatosensory evoked potentials, high-spatial-resolution MR imaging, and histopathologic analysis, concluding that rat studies of the weight-drop method "can serve as an adequate animal model for research on functional and morphologic changes after SCI and the effects of new treatment strategies" (9). In many respects, these authors augmented and supported the extensive work of others documenting the clear value of this model. However, to obtain MR images of considerably lower spatial resolution than those achieved in human subjects with a meter-bore 1.0-T system, the authors used a 4.7-T magnet with a 31-cm bore in rats. The focus of that study was chronic injury, whereas our study focus was acute injury. Chronic injury comprised mainly cystic changes, and areas of high signal intensity were shown to correspond to the cysts. Otherwise, the human and rat images were not comparable in terms of the meaning of the signal intensity changes or the quality of the detail shown between species. Also, Bilgen and Narayana (10) demonstrated intense CSF enhancement (ie, in the subarachnoid space) in rats after the intravenous administration of gadolinium in both injured and control spinal cords; this finding is distinctly different from that seen in humans, suggesting again that the two species are not fully analogous.

To eliminate the confounding effect of laminectomy and exposure of the spinal column to air, we developed a canine model of percutaneous translumbar compression SCI (8). We used a lumbar percutaneous approach to insert an angioplasty balloon and advance it to a level in the subarachnoid space adjacent to the spinal cord. In our previous series, 30-minute inflation of 4-mm balloons created less injury than did 7-mm balloons. Apart from researching the imaging features of SCI, other potential applications of the model in SCI research must still be systematically investigated.

In the present study, we sought to create a better scale for grading histopathologic injury and to better investigate the effects of balloon size and inflation time on the degree of injury, seeking also a balloon size that creates no injury. Therefore, the aim of this study was to determine the MR imaging characteristics of this model of graded compression SCI and to examine the correlation between the histopathologic findings and MR appearance of acute SCI. We hypothesized that the use of a greater variety of balloon sizes and that variation of compression times enables the creation of a gradation of injury varying from none to severe.

Methods

The study cohort included 17 male adult mongrel dogs weighing 18–36 kg. Six were from the original series of 30-minute inflations (8). All studies were performed with approval from our Institutional Animal Care and Research Advisory Committee.

All procedures followed the methods described previously (8). Briefly, after general endotracheal anesthesia was induced, we performed lumbar puncture perpendicular to the spinal canal via the lateral foramen under fluoroscopic guidance. Once the subarachnoid space was accessed, a guidewire was introduced and directed in a cephalad direction. Subsequently, techniques similar to those followed for angiography were used to advance an angioplasty balloon over the guidewire to the T6 vertebral level. After the position was verified fluoroscopically, balloon inflation was timed relative to the MR imaging time, such that approximately 30 minutes of the total 4-hour imaging session was spent during balloon inflation with the remainder spent for balloon deflation. Hence, in the case of 120- and 240-minute inflation times, balloons were inflated before the animals were transported to the MR unit. The animals remained under general anesthesia throughout imaging, at which time euthanasia was performed without awakening the animals from anesthesia. Each animal underwent a total of 4 hours of imaging, including both balloon inflation and deflation. The animals were then returned to the animal laboratory, where autopsy was performed to remove the spinal cord and to place it in formalin for subsequent histopathologic examination.

Before they were placed in the magnet, the animals were monitored with electrocardiography and pulse oximetry. We monitored the following physiologic measures: rectal temperature, oxygen saturation with an oximeter placed on the tongue, and pulse rate with continuous electrocardiographic recording. Oximeter recordings were not available during MR imaging examination, so oxygenation measures were reliably obtained only during balloon placement and transport to the MR unit. However, ventilator settings were maintained at approximately 20 respirations per minute throughout the experiment with a mixture of isoflurane and oxygen (approximately 2 L/min) added to room air. After their placement on the magnet, we were able to monitor only their heart rate. The animals were mechanically ventilated with a mixture of oxygen and fluothane throughout the experiment. Neuromuscular blockade was maintained pharmacologically. Blood pressures and blood glucose levels were not recorded.

For imaging, the animal was placed in the left lateral decubitus position. A linear-type, flexible surface coil of 9-inch circular diameter (C-1 coil; Philips, Best, the Netherlands) was located on the marked region of the spinal column overlying the balloon catheter. Images of the spinal region were acquired in the coronal, axial, and sagittal planes encompassing the region 1 cm above and below the balloon. T1-weighted images (TR/TE, 600/13; section thickness, 4 mm; intersection gap, 0.4 mm) were obtained during inflation of the balloon to confirm its location and to calculate the percentage of SCO. T1- and T2-weighted (2227/85; section thickness, 4 mm; intersection gap, 0.4 mm) as well as short-tau inversion recovery (STIR) images (TR/TE/TI, 1300/30/50; section thickness, 4 mm; intersection gap, 0.4 mm) were obtained after deflation of the balloon. Following the intravenous administration of gadopentetate dimeglumine 0.2 mmol/kg, T1-weighted images were

TABLE 1: Compression time, balloon diameter, and histologic and MR imaging results

Animal	Compression Time (min)	Balloon Size (mm)	H&E Grade*	βAPP Grade*	MR Imaging[†]				SCO (%)
					Enhancement	STIR	T1	T2	
1	30	4	0	0	0	None	−	−	29
2	30	4	0	2	0	None	+	−	31
3	30	7	3	3	1	None	−	−	79
4	30	7	2	3	0	None	−	−	62
5	30	7	3	0	1	None	+	−	67
6	30	7	3	0	0	+	+	−	69
7	120	2	0	0	0	−	−	−	12.5
8	120	2	0	0	0	−	−	−	20
9	120	4	2	2	1	+	−	−	38
10	120	4	0	0	0	−	−	−	28
11	120	4	0	2	1	+	−	+	43
12	120	7	2	0	1	+	−	−	78
13	240	4	3	0	1	+	−	−	56
14	240	4	3	1	1	+	−	−	44
15	240	7	3	0	1	+	−	−	82
16	240	2	0	0	0	−	−	−	17
17	240	2	0	0	0	−	−	−	12

*Subjective grading system: 0 indicates none; 1, mild; 2, moderate; and 3, severe.

T1 indicates T1-weighted; T2, T2-weighted; +, positive; −, negative.

acquired to evaluate contrast enhancement in the spinal cord. The entire MR imaging time was 4 hours, and the enhanced images were acquired near the end of the imaging session.

All balloons were 2 cm in length and 2, 4, or 7 mm in diameter. The earliest portion of the study was 30-minute balloon inflation, and only 4 and 7 mm balloons were used with that inflation time. In all animals, the balloons were inflated with a dilute solution of contrast material, and the degree of balloon expansion was evaluated on T1-weighted images.

For all MR images, balloon expansion was quantitatively assessed by using an offline software program (Functool 2000 Ra1.6; Sun Microsystems, GE Medical Systems, Milwaukee, WI) and axial T1-weighted images. SCO was determined by the ratio of the balloon area to the spinal canal area, expressed as percentage of occlusion. Images were assessed for indications of SCI, including increased signal intensity on T1- or T2-weighted images or STIR images and contrast enhancement.

On completion of MR imaging, the animal was euthanized and autopsied to remove the spinal cord. All spinal cords were placed in formalin and submitted for pathologic examination. Specimens were sectioned and processed with paraffin. The slides were stained with hematoxylin-eosin (H&E) to detect hemorrhage and immunostained with an antibody for neuronal beta amyloid precursor protein (βAPP) to detect axonal injury. Microscopic examination was subsequently performed. This technique was described previously (8). Severity of hemorrhage was graded as follows: Grade 1 was mild; grade 2, moderate; and grade 3, severe. Axonal injury was graded as follows: Grade 1 was pinpoint staining typically requiring high power for identification; grade 2, well-formed axonal swelling; and grade 3, severe or heavy staining. Two pathologists (C.L.W., R.R.R.) scored the histologic indications of injury without knowledge of the imaging findings.

The role of balloon diameter, degree of SCO, and duration of spinal cord compression was evaluated on the basis of indications of SCI on MR images and histopathologic examination. The sensitivity, specificity, and negative predictive value (NPV), and positive predictive value (PPV) of MR imaging were determined. Data analysis also included an evaluation of the statistical significance of any trends. With SCO as a dependent variable, one-way analysis of variance was used, with a linear contrast to assess the trend. Post hoc testing used contrasts, and P values were adjusted for multiplicity of testing. For ordered categorical variables, the Jonckheere-Terpstra trend

test was used. Relationships between dichotomous variables were examined by using the Fisher exact test. Observed significances exceeding .05 were considered not to be statistically significant. Data are presented as the mean ± SEM.

Results

All animals survived to complete the 4 hours of imaging. No animals had spinal cord laceration or other evidence of injury below the level of balloon inflation that would suggest injury from the catheterization. T1- and T2-weighted images of the spinal cord were acquired in all animals. STIR sequences were performed only in animals undergoing 120- or 240-minute inflation. Balloon inflations were successfully achieved in all animals. Results of 30-minute inflations were reported previously (8). Table 1 shows the diameter of the balloons and the duration of inflation for each animal.

SCO ranged from 12–20% with 2-mm balloons, 28–56% with 4-mm balloons, and 62–82% with 7-mm balloons. There was a significant trend for increasing SCO with increasing balloon diameter, with $F(1,14) = 114.1$ and $P < .0001$ (Fig 1). Post hoc testing showed differences among all balloon sizes.

Results of physiologic monitoring revealed that mean oxygen saturation per animal ranged from 96–99%, with a mean of 7.2 observations per animal when it could be observed. Individual observations were as low as 81% in one animal and 89% in two others, although mean values in each animal were in the range just described. Mean temperature recordings were 99°F, ranging from 98.75°F to 101°F, with a mean of 6.3 (range, 1–12) observations per animal. Heart rates ranged from a mean of 99.5 to 127 beats per minute (bpm), with an overall mean of 117.2 bpm and an average of 11 (range, 8–15) observations per animal. The lowest observed heart rate was 80 bpm. One animal had
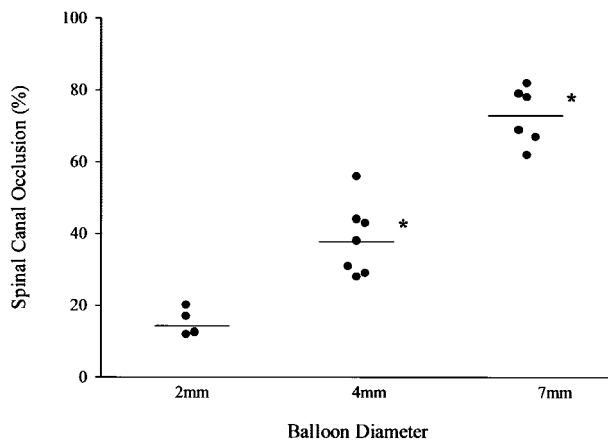
FIG 1. Each increase in balloon size produced a statistically significant (*asterisk*) increase in the percentage of SCO.

a single recording as high as 175 bpm, with recordings of 125 bpm before and after this.

Histopathologic examination did not show abnormal staining of the spinal cord in animals that received a 2-mm balloon. Evidence of hemorrhage or axonal injury was detected in five of seven animals with 4-mm balloons: Two had both axonal injury and hemorrhage, two had axonal injury, and one had hemorrhage (Figs 2 and 3). Evidence of hemorrhage was seen in all animals with 7-mm balloons and axonal injury was detected in two. Table 1 shows the grades of hemorrhage and axonal injury. All animals with SCO >29% had histopathologic findings of hemorrhage or axonal injury (Fig 4). Hemorrhage or axonal injury was observed with all durations of spinal cord compression with a 7-mm balloon but not with 2-mm balloons. With 4-mm balloons, the percentage of animals with histologic abnormalities increased from 50% to 100% as the duration of compression increased from 30 to 240 minutes. SCO percentage increased with increasing hemorrhage grade, with $F(1,14) = 32.5$ and $P < .0001$. Post hoc testing indicated that the percentage of grade 2 SCO was higher than that of grade 0; however, the percentage of grade 3 SCO was not significantly larger than that of grade 2. Grade of hemorrhage also increased with balloon size ($P = .002$). Grade axonal injury was not significantly correlated with SCO percentage or balloon size.

MR imaging depicted indications of SCI in 10 of 11 animals with histologic evidence of SCI. MR images showed a normal spinal cord in all animals with a 2-mm balloons. Abnormal MR findings were documented in six of the seven animals with 4-mm balloons and in five of the six animals with 7-mm balloons. No abnormalities were documented by MR imaging and histopathologic findings in animals with SCO <29%. For all durations of spinal cord compression, MR images documented histopathologic findings of SCI in most animals with 4- (86%) and 7-mm (83%) balloons. No injuries occurred with 2-mm balloons, and no false-positive MR studies were noted. The only false-negative MR study predated our use of

the STIR sequence. In the 11 animals with histopathologic evidence of SCI, T1-weighted images depicted SCI in three, T2-weighted images depicted SCI in one, and contrast-enhanced T1-weighted images showed enhancement in eight (Fig 5). STIR images were acquired in 12 animals and showed increased signal intensity in all animals with histologic evidence of SCI (Fig 6). Table 2 shows the sensitivity, specificity, and PPV, and NPV of MR imaging. Findings of contrast enhancement and on STIR images were associated with hemorrhage (each $P = .01$). No CSF enhancement was seen.

Discussion

In exploring SCI, there are many directions that may lead to important discoveries and progress. Clearly, much has been learned from literally hundreds of studies in rodents over the last several years. Many studies are enabled by use of small animals that will permit large numbers of subjects, and repeated studies in many laboratories contribute to the validation of results. Furthermore, with advances in small-bore high-field-strength MR technology, it is now feasible to perform some imaging studies in small animals and to compare findings with those of human studies. However, there are large gaps in the information needed for the diagnostic assessment, day-to-day care, and long-term follow-up and therapeutic assessment of SCI.

Humans cannot be imaged in small-bore magnets or routinely imaged in high-field-strength magnets. The resolutions available for imaging live rodent spinal cords with high-field-strength magnets and the variety of sequences used to image human injury in clinical magnets are not fully analogous. A different model is needed to examine clinically relevant imaging parameters in a clinically relevant system to optimize the care we can deliver to patients, even if that model is not ideal for practical exploration of the biology of SCI in large numbers of animals; we acknowledge the great advantage of using highly refined manipulations of experimental parameters in small-animal models. More studies are needed, including survival studies with further establishment of clinical parameters in the canine model; however, the species has self-evident and undeniable advantages insofar as the spinal cord is similar to the human spinal cord in terms of imaging and the standard clinical systems used to study it.

Furthermore, while small-animal models with large numbers of subjects are highly appropriate for some interventions (involving drugs, etc), the availability of an animal model in which those interventions can be practiced assists the development of technologies to achieve those interventions. Just as much progress has been made in cardiology and in neurovascular work with canine and porcine models because these models have arteries large enough to catheterize, as the rodent spinal canal is inappropriate for experimentation with devices and techniques that might be used in humans. For example, using the percutaneous
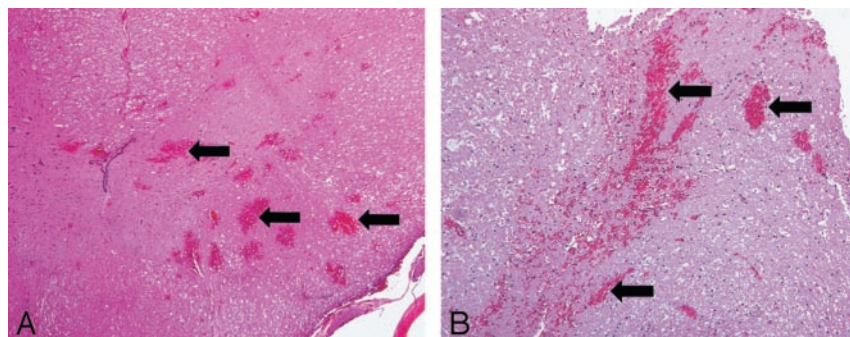
FIG 2. SCI on H&E stains. Grades were subjectively based on density and cross-sectional hemorrhagic involvement, where no hemorrhage was grade 1. *Arrows* indicate areas of hemorrhage.
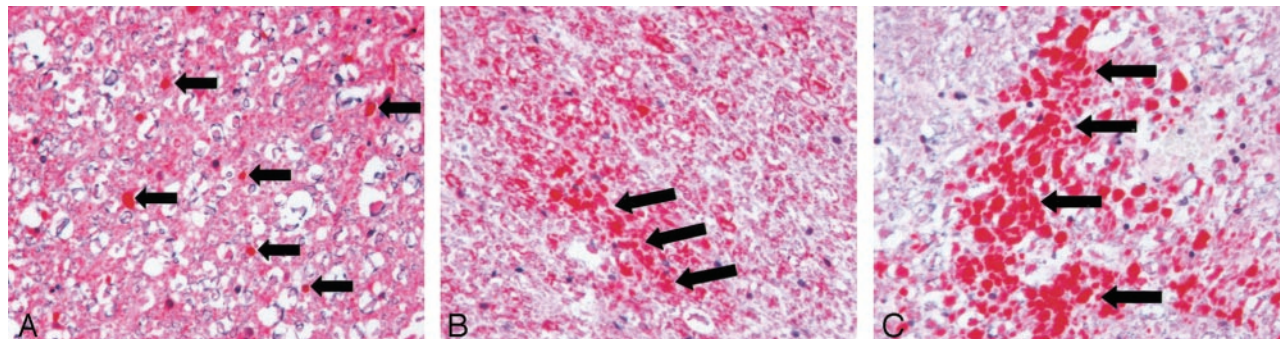 *A*, Grade 2 injury, animal 4.
  B, Grade 3 injury, animal 14.

FIG 3. SCI on βAPP stains. *Arrows* indicate areas of axonal accumulation of stain. Note increasing axonal staining with increasing grades of injury.
  A, Grade 1 injury, animal 14.
  B, Grade 2 injury, animal 2.
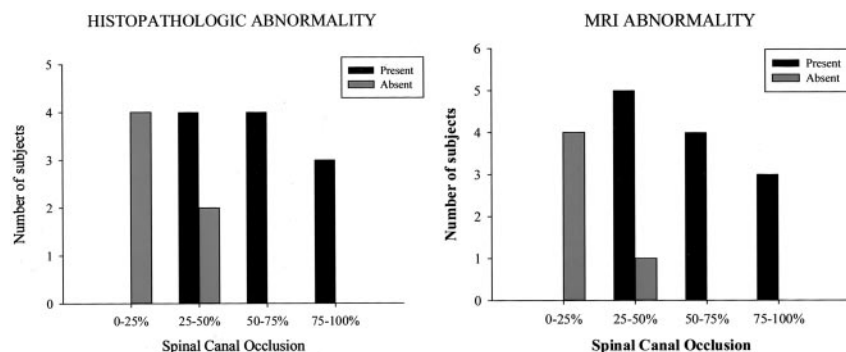 *C*, Grade three injury, animal 4.

FIG 4. Changes as SCO increases. Sample sizes were too small to achieve statistical significance, particularly because all animals with occlusion of 50% or greater had abnormal MR imaging and histopathologic findings.
  A, Histopathologic abnormality.
  B, MR imaging abnormality.

intraspinal navigation technique (11), we demonstrated the ability to navigate the entire spinal canal from a lumbar puncture in human cadavers. Techniques such as local drug introduction, hypothermic lavage, or even stem cell implantation may be feasible in brain or spinal cord by using this technique. However, the technique, with its tools, could never be developed in a rat, and exploration of spinal cord interventions with this approach and with tools that could realistically be used in humans is impossible if all other models are rejected as valueless.

This argument need not be interpreted as a denial of the validity of the weight-drop method or of rodent studies. Those approaches are simply not comprehensive enough to render other models valueless, and by the nature of the differences between the species (humans vs rats) and the technologies necessarily applied in previous studies, they cannot be made comprehensive. On the other hand, rodent models are certainly more developed at present, and greater work is required to validate a larger animal model; such work includes functional outcome studies, electrophysiologic studies, and long-term histopathologic studies and correlations with imaging, among others. The present study simply demonstrates the potential for an intermediate model between rats and humans that is relatively less invasive, certainly more analogous in the technologies applied, and potentially amenable to experimentation with percutaneous therapeutic interventions with techniques that could not be performed in rodents.

This model is also not the first in canines or the first to use balloons. Some authors (12, 13) have used epidural balloons placed by means of limited laminectomy and then advanced a short distance in the epidural space before inflation to create compression. Others (14) have used a Teflon screw placed in the cervical spine. To our knowledge, our model is the
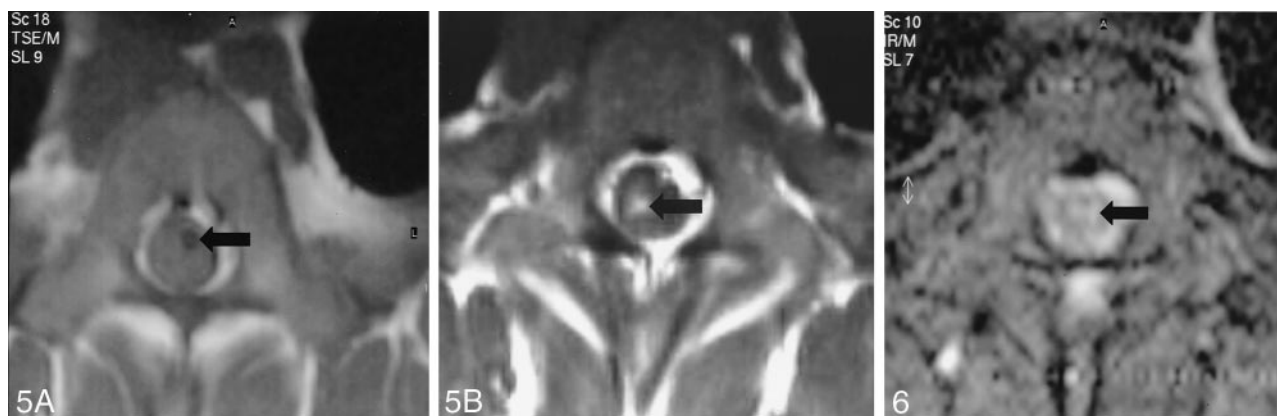
Fig 5.   T1-weighted images in animal 14 show no injury before contrast enhancement but enhancement in the spinal cord (*arrow*) after administration of gadolinium contrast agent.
  A, Nonenhanced image. *Arrow* indicates the deflated balloon.
  B, Gadolinium-enhanced image.

Fig 6.   Axial STIR image in animal 12, which showed no findings of hemorrhage on H&E stains but grade 2 injury on βAPP stains. Note the central increase in signal intensity in the spinal cord (*arrow*).

TABLE 2: Sensitivity, specificity, and PPV, and NPV of MR imaging

Sequence	Sensitivity (%)	Specificity (%)	PPV (%)	NPV (%)
Enhanced	64	100	100	60
STIR	100	100	100	100
T1- and T2-weighted	45	83	83	50

first in which the balloon is passed through the subarachnoid space. Although epidural balloon placement is obviously feasible and may be worthy of further investigation, use of the subarachnoid space permits notable control over balloon placement, it allows the percutaneous creation injury with well-understood techniques, and it provides a potential pathway for navigation during treatment as well as injury creation. Therefore, our selection of the subarachnoid space was based on its positive advantages and not a rejection of prior work.

In our previous report (8), we described the results of 30-minute compression without statistical comparison with the longer compression times, without the use of 2-mm balloons, and without use of the grading scale for histologic injury. Regarding this initial group, we were disappointed with the sensitivity of MR imaging in detecting acute injury and therefore added STIR imaging to the animals undergoing longer compression. In the present expanded series, we further examined the effect of the degree and duration of spinal cord compression on MR findings of the spinal cord and also performed histopathologic assessment. No therapeutic interventions were introduced, although survival studies must still be performed; however, the demonstration of graded injury based on inflation time and balloon diameter—including the finding that the smallest balloon created no injury even at long inflation times (thus forming a control group)—notably expands and validates earlier results.

In weight-drop models, the intensity of injury in experimental spinal cord trauma is controlled by ad-

justing weight of the mass and the height from which it is dropped (15–18). The present findings showed that graded spinal cord compression, as measured by SCO, can be accomplished by using the percutaneous translumbar technique. With varying balloon sizes, SCOs ranging from 12–82% were created. SCO significantly increased as larger balloons were used. We also examined the effect of the duration of spinal cord compression on the creation of SCI. As Anderson and Stokes (6) suggested in their review, the spinal cord may have no permanent deficits when slow compression is applied. Although the rate of balloon inflation was kept the same for each balloon size, we applied spinal cord compression for 30–240 minutes using a 4-mm balloon. Although our number of subjects was too small to achieve significance regarding compression time with this balloon size, we observed a strong trend toward more reliable and severe injury with longer inflation times. Delineation of the effect of compression time on the spinal cord warrants further evaluation in a larger series to better identify the applicability of this model in the neuroscience of SCI.

The correlation of MR findings to clinical and pathologic findings has been of interest to several investigators. Using weight-drop models, some have suggested that lesion length and hyperintense and hypointense areas on MR images are reliable indicators of the severity of trauma (15, 16, 19). In the present study, histopathologic and MR findings documented no abnormalities in subjects with SCO <30%. Increasing balloon size significantly increased SCO and hemorrhage. The sensitivity and specificity of MR imaging varied in the detection of SCI. Combined T1- and T2-weighted findings had the lowest diagnostic performance. Contrast enhancement and STIR sequences provided a specificity of 100%; however, the sensitivity of contrast enhancement (64%) did not match that achieved with STIR imaging (100%). Furthermore, STIR imaging provided excellent PPV and NPV. In a previous study of a weight-drop model in canines, T2-weighted imaging depicted

abnormal signal intensity better than did T1-weighted 0.5-T sequences (15). A STIR sequence was not tested in that study. These investigators created four grades of trauma; however, the model was not perfectly reproducible, as the spinal cord lesions were not identical when similar degrees of trauma were induced. All subjects had hemorrhage and edema, as shown on pathologic specimens, and the overall signal intensity on T2-weighted images had the same grade of abnormality. Nevertheless, our results and those of the previous weight-drop study must be interpreted in light of the small number of subjects and also the differences in the magnetic field strengths used. Our findings showed that the percutaneous translumbar model of spinal cord compression can potentially be used to investigate the diagnostic performance of MR images.

Similar to the studies using the weight-drop model (17–19), our histopathologic examination demonstrated the creation of graded injury. Hemorrhage or axonal injury was present in all subjects with SCO >29%. The present findings also indicated that the frequency of detected hemorrhage or axonal injury increased with greater balloon diameter. Axonal injury is one of the pathologic processes in SCI, and we detected the presence of axonal injury by using βAPP staining. βAPP is a glycoprotein that accumulates in axons when the axonal transport is disrupted. Previous studies have shown the aggregation of βAPP in human and nonhuman spinal cord exposed to compression injury (20–23). Although the grade of axonal injury was not significantly correlated with SCO percentage and balloon size, βAPP was commonly present when STIR images showed abnormal signal intensity not detected on T1- and T2-weighted images. This finding may be of value in assessing patients with SCI. As Quencer et al (24) showed, MR imaging and pathologic observations indicate that acute traumatic central cord syndrome is predominantly a white matter injury and hemorrhage is an uncommon finding. Furthermore, some patients with SCI are known to have neurologic improvement, which cannot be explained by the resolution of edema on T2-weighted images (24). A plausible explanation for this neurologic improvement is possible myelin repair at the myelin-axon units. On the basis of our findings, one can speculate that STIR images may be useful for detecting axonal injury in patients with less severe injury. STIR imaging has already been reported to improve sensitivity in detecting demyelinating lesions of the spinal cord, especially in patients with multiple sclerosis (25–27). The role of STIR imaging in detecting graded SCI merits further investigation. Many points can be made about this model, including the value of larger animal models for studying imaging findings in this disease. To our knowledge, studies comparable to ours have not been done and cannot be done in rodents or other small animals, particularly if MR devices applicable to human studies (eg, 1.5-T meter-bore magnets) are used.

The grading scale used for histopathologic assessment needs further refinement in larger numbers of subjects. The heterogeneity of injuries in this study corresponds to that seen in human injury and complicates true quantification in this small series. Quantification of injury based on the extent of injury in cross-section may be feasible, but it is compounded by length of injury along the spinal cord, and vice versa. The subjective grading of injury in this study illustrates the problem rather than solves it, and a more reproducible and quantified means is needed to account for multiple factors; this will make the analysis more complex and thereby more difficult to replicate between institutions. Nonetheless, the lack of quantitation is a shortcoming of this method. Clinical correlation with the degree of injury is another important area for future study, but it was beyond the scope of this work. Also, the greater correlation between the degree of occlusion and the injury seen in hemorrhagic versus axonal injury is interesting, but a larger series is needed to draw conclusions about that observation. Longer survival after injury may increase the observed axonal injury as well.

The purpose of this study was to determine our ability to create graded injuries in this model; still, more complete physiologic monitoring would have enhanced our understanding of underlying pathophysiologic mechanisms of the injury. On the basis of the physiologic data collected, we do not believe that hypoxia, hypothermia, hyperthermia, or bradycardia contributed to the injury. However, more thorough monitoring of blood pressure and blood glucose levels are warranted in subsequent studies.

Also, the relative contributions of ischemia and direct compressive trauma are difficult to study because the compression is generally thought to be the cause of the ischemia. However, assessment of the contributions of direct compression and reperfusion injury may be possible by using techniques such as diffusion-weighted imaging or direct perfusion imaging. These topics are worthy of further investigation but were not part of this study.

Conclusion

Graded degrees of SCI can be achieved in dogs by varying the sizes of balloons or by varying the times of inflation in the percutaneous translumbar technique described herein. Whereas 2-mm balloons produce no injury and 7-mm balloons always produce injury, 4-mm balloons seem to create injury that increases with rising inflation times. However, the study did not find significant differences for inflation time, and the data only support the conclusion that the degree of compression seems to be more important than the time of compression.

An investigation of imaging parameters for SCI is needed to understand how to optimize care. This study did not evaluate clinical parameters or treatment methods in SCI. However, our finding of improved sensitivity with STIR sequences shows the applicability of models of larger animals in studies of imaging parameters. As more sophisticated therapies emerge, better imaging techniques are needed to op-

timize visualization of the therapeutic results. Technology equivalent to that used in human studies will assist these types of translational studies.

References

1. Allen AR. **Surgery of experimental lesion of spinal cord equivalent to crush injury of fracture dislocation of spinal column: a preliminary report.** *JAMA* 1911;878–880
2. Anderson TE. **A controlled pneumatic technique for experimental spinal cord contusion.** *J Neurosci Methods* 1982;6:327–333
3. Anderson TE. **Spinal cord contusion injury: Experimental dissociation of hemorrhagic necrosis and subacute loss of axonal conduction.** *J Neurosurg* 1985;62:115–119
4. Ridella SA, Anderson TE. **Compression of rat spinal cord in vitro: effects of ethanol on recovery of axonal conduction.** *Cent Nerv Syst Trauma* 1986;3:195–205
5. Kobrine AI, Evans DE, Rizzoli HV. **Experimental acute balloon compression of the spinal cord: factors affecting disappearance and return of the spinal evoked response.** *J Neurosurg* 1979;51:841–845
6. Anderson TE, Stokes BT. **Experimental models for spinal cord injury research: physical and physiologic considerations.** *J Neurotrauma* 1992;9:S135–S142
7. Bilgen M, Narayana PA. **A pharmacokinetic model for quantitative evaluation of spinal cord injury with dynamic contrast-enhanced magnetic resonance imaging.** *Magn Reson Med* 2001;46:1099–1106
8. Purdy PD, Duong RT, White CL III, et al. **Percutaneous translumbar spinal cord compression injury in a dog model using angioplasty balloons: MR imaging and histopathologic findings.** *AJNR Am J Neuroradiol* 2003;24:177–184
9. Metz GAS, Curt A, van de Meent H, Klusman I, Schwab ME, Dietz V. **Validation of the weight-drop contusion model in rats: a comparative study of human spinal cord injury.** *J Neurotrauma* 2000;17:1–17
10. Bilgen M, Narayana P. **A pharmacokinetic model for quantitative evaluation of spinal cord injury with dynamic contrast-enhanced magnetic resonance imaging.** *Magn Reson Med* 2001;46:1099–1106
11. Purdy PD, Replogle RE, Pride GL Jr, Adams C, Miller S, Samson D. **Percutaneous intraspinal navigation (PIN): A feasibility study in cadavers of a new and minimally invasive approach to the spinal cord and brain.** *AJNR Am J Neuroradiol* 2003;24:361–365
12. Griffiths IR. **Vasogenic edema following acute and chronic spinal cord compression in the dog.** *J Neurosurg* 1975;42:155–165
13. Hansebout RR, van der Jagt RH, Sohal SS, Little JR. **Oxygenated fluorocarbon perfusion as treatment of acute spinal cord compression injury in dogs.** *J Neurosurg* 1981;55:725–732
14. Al-Mefty O, Harkey L, Marawi I, et al. **Experimental chronic compressive cervical myelopathy.** *J Neurosurg* 1993;79:550–551
15. Schouman-Claeys E, Frija G, Cuenod CA, Begon D, Paraire F, Martin V. **MR imaging of acute spinal cord injury: Results of an experimental study in dogs.** *AJNR Am J Neuroradiol* 1990;11:959–965
16. Hackney DB, Ford JC, Markowitz RS, Hand CM, Joseph PM, Black P. **Experimental spinal cord injury: MR correlation to intensity of injury.** *J Comput Assist Tomogr* 1994;18:357–362
17. Noble LJ, Wrathall JR. **Spinal cord contusion in the rat: morphometric analyses of alterations in the spinal cord.** *Exp Neurol* 1985;88:135–149
18. Wrathall JR, Pettegrew RK, Harvey F. **Spinal cord contusion in the rat: production of graded, reproducible, injury groups.** *Exp Neurol* 1985;88:108–122
19. Weirich SD, Cotler HB, Narayana PA, et al. **Histopathologic correlation of magnetic resonance imaging signal patterns in a spinal cord injury model.** *Spine* 1990;15:630–638
20. Ahlgren S, Li GL, Olsson Y. **Accumulation of beta-amyloid precursor protein and ubiquitin in axons after spinal cord trauma in humans: immunohistochemical observations on autopsy material.** *Acta Neuropathol (Berl)* 1996;92:49–55
21. Li GL, Farooque M, Holtz A, Olsson Y. **Changes of beta-amyloid precursor protein after compression trauma to the spinal cord: an experimental study in the rat using immunohistochemistry.** *J Neurotrauma* 1995;12:269–277
22. Li GL, Farooque M, Holtz A, Olsson Y. **Effects of alpha-phenyl-N-tert-butyl nitrone (PBN) on compression injury of rat spinal cord.** *Free Radical Res* 1997;27:187–196
23. Westergren H, Yu WR, Farooque M, Holtz A, Olsson Y. **Systemic hypothermia following spinal cord compression injury in the rat: Axonal changes studied by beta-APP, ubiquitin, and PGP 9.5 immunohistochemistry.** *Spinal Cord* 1999;37:696–704
24. Quencer RM, Bunge RP, Egnor M, et al. **Acute traumatic central cord syndrome: MRI-pathological correlations.** *Neuroradiology* 1992;34:85–94
25. Hittmair K, Mallek R, Prayer D, Schindler EG, Kollegger H. **Spinal cord lesions in patients with multiple sclerosis: Comparison of MR pulse sequences.** *AJNR Am J Neuroradiol* 1996;17:1555–1565
26. Campi A, Pontesilli S, Gerevini S, Scotti G. **Comparison of MRI pulse sequences for investigation of lesions of the cervical spinal cord.** *Neuroradiology* 2000;42:669–675
27. Bot JC, Barkhof F, Lycklama a Nijeholt GJ, et al. **Comparison of a conventional cardiac-triggered dual spin-echo and a fast STIR sequence in detection of spinal cord lesions in multiple sclerosis.** *Eur Radiol* 2000;10:753–758